Interdependence between Structural Engineering and Construction Management
Edited by Ozevin, D., Ataei, H., Modares, M., Gurgun, A., Yazdani, S., and Singh, A.

ISBN: 978-0-9960437-6-2

FINITE STRAIN MEASUREMENT USING IMAGE ANALYSIS UNDER REVERSE SHEAR AFTER FORWARD SHEAR

YASUYUKI KATO

Dept of Mechanical Engineering, Nihon University, Tokyo, Japan

The purpose of this research is to investigate the progress of local deformation under finite deformation by using image analysis based on the Natural Strain theory. Since Natural Strain used in the image analysis can satisfy the addition law of strain on an identical line element and can remove the rigid body rotation from shearing strain component, it is an effective strain for representing stress and strain behavior under large deformation. Therefore, in this research, these features of Natural Strain theory will be incorporated into the method of image analysis. In the present study, using the test pieces made of high purity tough pitch copper, the local deformation occurring under large simple shear is investigated by comparing the strains in each element from the upper position to the middle position with the average strain in the gauge length. In order to investigate the progress of local deformation caused by differences of strain hardening in the material, the experiments are conducted under different deformation histories which are given by applying reverse shear after applying forward shear with different sizes. Consequently, it is revealed that if the value of plastic strain obtained by integrating over the whole deformation path is almost the same, the progress of local deformation is approximately the same even if the deformation path is different.

Keywords: Finite deformation, Elasto-plasticity, Large deformation, Natural strain, Plastic strain, Deformation path, Ductile metal.

1 INTRODUCTION

In general, the electrical measurements such as displacement meter and strain gauge have been widely used for the finite strain measurements. Among these measurements, if one considers the case that the strain gauge is used, the strain gauge is peeled off with an increase of deformation. Hence, there is a limit in the range that it can be measured continuously. On the other hand, in the case of using image analysis, it is possible to measure the strain continuously over the wide range from the infinitesimal deformation to the large deformation. Moreover, the measurement by conventional displacement meter is an average strain in the gauge length of the test piece. On the other hand, in the case of using image analysis, it is possible to measure the strain directly at the position where the picture image is taken. Hence, the measurement by image analysis is very effective for local strain measurements. In this research, using the features of Natural Strain theory effectively into the image analysis, the progress of local deformation under large simple shear is investigated. The Natural Strain theory used in this research is the strain expression which is obtained by integrating the infinitesimal strain increment on an identical line element over the whole process of deformation path (Kato and Moriguchi 2003). Consequently, since the

shearing strain component of Natural Strain is defined by pure angular strain, the rigid body rotation can be removed completely from the shearing strain component. Moreover, since the addition law of strain can be satisfied, it is possible to represent subsequent strain by adding the strain from anywhere with reference to the deformed intermediate state.

In our previous study (Kato and Futami 2013), in order to confirm the accuracy of this image analysis, the experiments of three types of different deformation paths, i.e., the proportional loading of tension and shear, the shear after applying tension and the tension after applying shear, were conducted. In those experiments, strain measurements by the image analysis have been compared with measurements by conventional displacement meter, and the validity of this image analysis has been verified. However, in these studies, experiments have been done in the range of uniform deformation fields where the local deformation does not still occur. Hence, as for the larger deformation after local deformation began to occur, detailed measurements have not been done yet in our previous study. Therefore, in the previous report (Kato 2015), the progress state of local deformation with respect to the uniaxial state such as tension or shear has been investigated.

Moreover, in the present study, in order to examine the progress of local deformation in more detail, the experiments are conducted under the different deformation paths which are given by applying the reverse shear after applying the forward shear with different sizes. Then, the relation between the developmental process of local deformation and the deformation history of simple shear is revealed.

2 MEASUREMENT METHOD OF PRINCIPAL STRAIN AND LOCAL DEFORMATION

The Figure 1 (a) shows the three-line elements ℓ_{oa}, ℓ_{ob}, ℓ_{oc} which are located at arbitrary directions $\beta_{oa}, \beta_{ob}, \beta_{oc}$. Among these line elements, if we consider a line element ℓ_{oa}, the relation between original un-deformed state and deformed current state of the line element can be derived as in Eq. (1),

$$\ell_a = \boldsymbol{D}\,\ell_{oa} = \begin{bmatrix} D_{11} & D_{12} \\ 0 & D_{22} \end{bmatrix} \begin{bmatrix} \|\ell_{oa}\| \cos\beta_{oa} \\ \|\ell_{oa}\| \sin\beta_{oa} \end{bmatrix} \tag{1}$$

where, $\boldsymbol{D}$ is a deformation gradient tensor. In this instance, the extensional strain component of the Natural Strain theory is expressed by Eq. (2),

$$\varepsilon_a = \frac{1}{2} ln\left(\frac{\ell_a{}^T \ell_a}{\ell_{oa}{}^T \ell_{oa}} \right) = \frac{1}{2} ln\left(\frac{\ell_{oa}{}^T \boldsymbol{D}^T \boldsymbol{D} \ell_{oa}}{\ell_{oa}{}^T \ell_{oa}} \right) = \frac{1}{2} ln\left(D_{11}{}^2 cos^2\beta_{oa} + 2D_{11}D_{12} sin\beta_{oa} cos\beta_{oa} + D_{12}{}^2 sin^2\beta_{oa} + D_{22}{}^2 sin^2\beta_{oa} \right) \tag{2}$$

Similarly, the extensional strain components for other line elements, i.e., ε_b and ε_c, can also be derived. Hence, the following relation is obtained (Kato and Futami 2013).

$$\begin{bmatrix} D_{11}{}^2 \\ D_{11}D_{12} \\ D_{12}{}^2 + D_{22}{}^2 \end{bmatrix} = \begin{bmatrix} cos^2\beta_{oa} & 2\sin\beta_{oa}\cos\beta_{oa} & sin^2\beta_{oa} \\ cos^2\beta_{ob} & 2\sin\beta_{ob}\cos\beta_{ob} & sin^2\beta_{ob} \\ cos^2\beta_{oc} & 2\sin\beta_{oc}\cos\beta_{oc} & sin^2\beta_{oc} \end{bmatrix}^{-1} \begin{bmatrix} exp(2\varepsilon_a) \\ exp(2\varepsilon_b) \\ exp(2\varepsilon_c) \end{bmatrix} \tag{3}$$

As shown in Figure1 (c), if we consider the special case that the line element ℓ_{oa} is fixed on the base surface in an initial state, i.e., $\beta_{oa} = 0$, $\beta_{ob} = \beta_{oa} + \pi/4$, $\beta_{oc} = \beta_{oa} + \pi/2$, the components of deformation gradient tensor are represented through Eq. (4-6).

$$D_{11} = exp(\varepsilon_a) \tag{4}$$

$$D_{12} = exp(2\varepsilon_b - \varepsilon_a) - \frac{1}{2}(exp(\varepsilon_a) + exp(2\varepsilon_c - \varepsilon_a)) \tag{5}$$

$$D_{22} = \sqrt{exp(2\varepsilon_c) - \left\{exp(2\varepsilon_b - \varepsilon_a) - \frac{1}{2}(exp(\varepsilon_a) + exp(2\varepsilon_c - \varepsilon_a))\right\}^2} \tag{6}$$

Moreover, the principal value of strain e_1 and its direction θ_m can be determined from the polar decomposition of deformation gradient, and these are represented in Eq. (7) and Eq. (8).

$$e_1 = ln\,\lambda_1 = ln\left\{\frac{\sqrt{D_{11}^2 + D_{12}^2 + D_{22}^2 + 2D_{11}D_{22}} + \sqrt{D_{11}^2 + D_{12}^2 + D_{22}^2 - 2D_{11}D_{22}}}{2}\right\} \tag{7}$$

$$\theta_m = \frac{\pi}{4} - \frac{1}{2}\,tan^{-1}\left\{\frac{D_{11}^2 + D_{12}^2 - D_{22}^2}{2\,D_{12}D_{22}}\right\} \tag{8}$$

In the present study, in order to evaluate the local deformation quantitatively, the differences of principal strain Δe_1 between the principal strain in each position in a test piece e_{1i} and the strain measured by displacement meter e_{1d} (see Eq. (9)) are measured.

$$\Delta e_1 = e_{1i} - e_{1d} \tag{9}$$

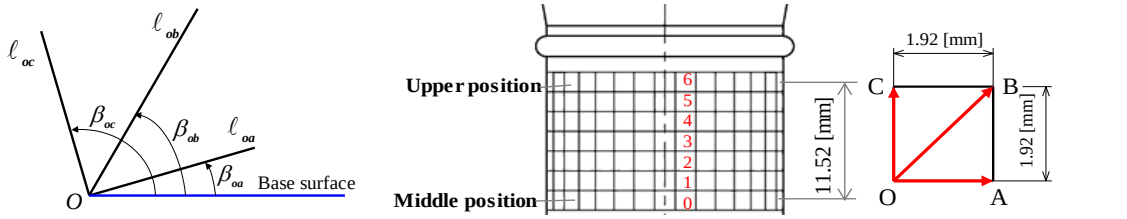

(a) Three line elements. (b) Position of elements. (c) Enlarged view of elements.

Figure 1. Measurement method of local deformation.

3 EXPERIMENTAL METHOD

3.1 Experimental Equipment and Test Specimen

Since it is necessary to keep the axial displacement zero during the process of applying a large simple shear, a multi-axial loading machine, which can apply the axial displacement and the shearing displacement at the same time, was used for conducting this experiment. As for the test piece used in experiments, hollow cylindrical specimens made from annealed high purity tough pitch copper, i.e., outer diameter 22 [mm], inner diameter 16 [mm] and gauge length 30 [mm] , are adopted. As shown in Figure 1 (b), in order to perform image measurements, scribe lines were preliminarily drawn with grid pattern (uniform interval 1.92 [mm]) on the surface of the test piece. Then, after attaching this test piece to the testing machine, the image measurement has been carried out by applying the torque with keeping the axial displacement zero. Here, the image measurements are performed on seven small elements (N=0~6) from the middle position to the upper position on the surface of a specimen (see Figure 1 (b)). The photographic camera used in this study is high pixel camera made from Canon (21.1 megapixel), and in order to measure the

deformation on an identical line element, the image photographs of each element, where the resolution is 0.0014 [mm/px], were measured by rotating the camera and moving it up and down.

3.2 Experimental Conditions

In this study, in order to examine the progress of local deformation, the strain measurements in each small element are conducted on the following different deformation paths:

(Ⅰ) Simple shear in forward direction only: extensional strain e_1 = 1.1 [-] (slip $K = D_{12}$ = 2.7 [-], torsional angle φ = 490 [deg.])

(Ⅱ) Simple shear in reverse direction after forward direction: e_1 = 0.7 [-] (K = 1.52 [-], φ = 275 [deg.]) ⇒ e_1 = - 0.2 [-] (slip K = - 0.34 [-], torsional angle φ = - 62 [deg.])

(Ⅲ) Simple shear in reverse direction after forward direction: e_1 = 0.5 [-] (K = 1.05 [-], φ = 190 [deg.]) ⇒ e_1 = - 0.6 [-] (slip K = - 1.27 [-], torsional angle φ = - 230 [deg.])

(Ⅳ) Simple shear in reverse direction after forward direction: e_1 = 0.3 [-] (K = 0.62 [-], φ = 114 [deg.]) ⇒ e_1 = - 1.0 [-] (slip K = - 2.36 [-], torsional angle φ = - 427 [deg.]).

4 EXPERIMENTAL RESULTS

The progress of local deformation under different deformation paths is firstly examined by comparing the results of image measurement at middle position with upper position. As one example of these experimental results, Figure 2 shows the result for deformation path Ⅱ. Here, Figure 2 (a) represents the relation of principal deviatoric stress and principal deviatoric strain. On the other hand, Figure 2 (b) shows the comparison of photographs of small elements taken at the place of middle and upper position in the test piece with respect to points a and c in Figure 2 (a). From comparison of photographs at the point c_0 and c_6, it can be confirmed that since the results of both images are different, the local deformation had already begun to occur. Similarly, Figure 3 shows the result of deformation path Ⅳ that the shear deformation in the forward direction is the smallest in these experiments. It is revealed from Figure 3 (a) that the local deformation begins to occur under larger reverse shear as compared with the result of deformation path Ⅱ.

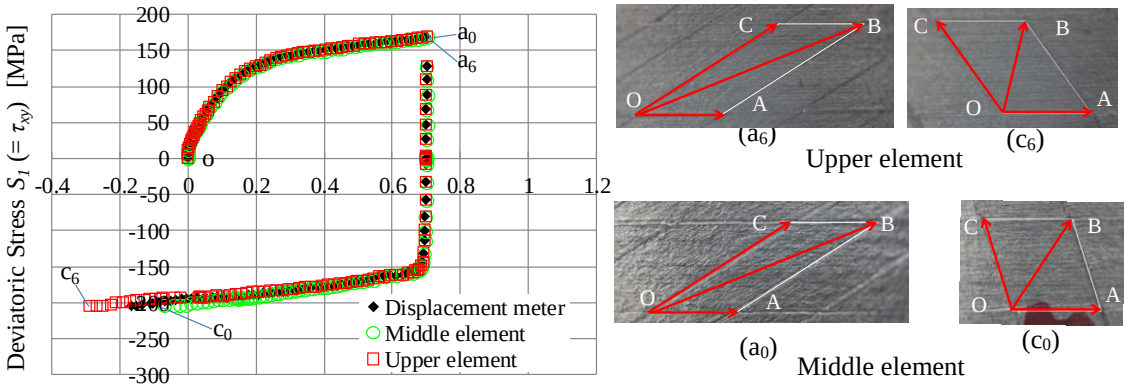

(a) Principal deviatoric stress and strain diagram. (b) Image photographs.

Figure 2. Simple shear in reverse direction after forward direction (deformation path Ⅱ).

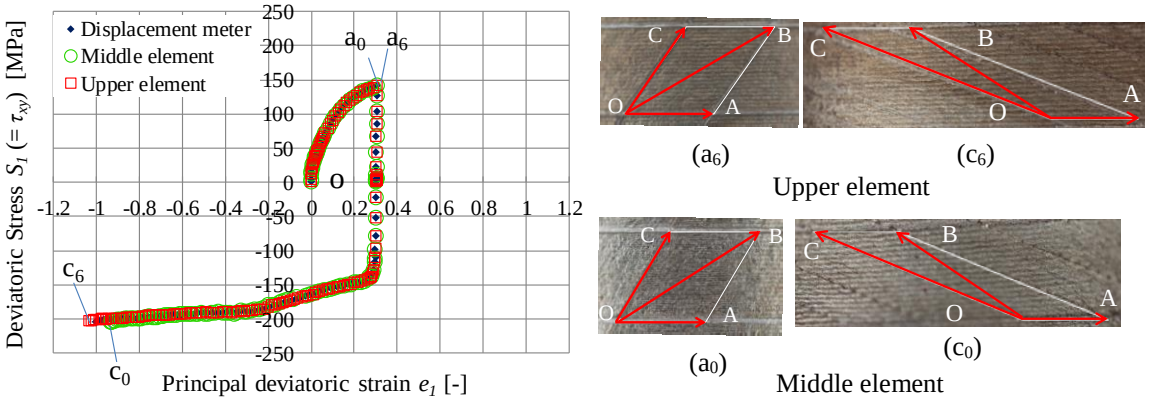

(a) Principal deviatoric stress and strain diagram. (b) Image photographs.

Figure 3. Simple shear in reverse direction after forward direction (deformation path Ⅳ).

Next, in order to confirm the progress of local deformation at each position in the test piece, the state of local deformation is investigated at a point b in Figure 4 (a) where the shear deformation measured by using the displacement meter becomes zero. Figure 4 (b) shows the distributions of the differences of principal strain Δe_1 definded by Eq. (9). In this Figure, as for the deformation path Ⅱ, which is the largest forward shear, it can be comfirmed that since the distribution of Δe_1 changes from a plus through zero to minus, the local deformation has already occurred. On the other hand, as for the case of deformation path Ⅲ and Ⅳ, since the distributions of Δe_1 show little change, the local deformation has not yet occurred.

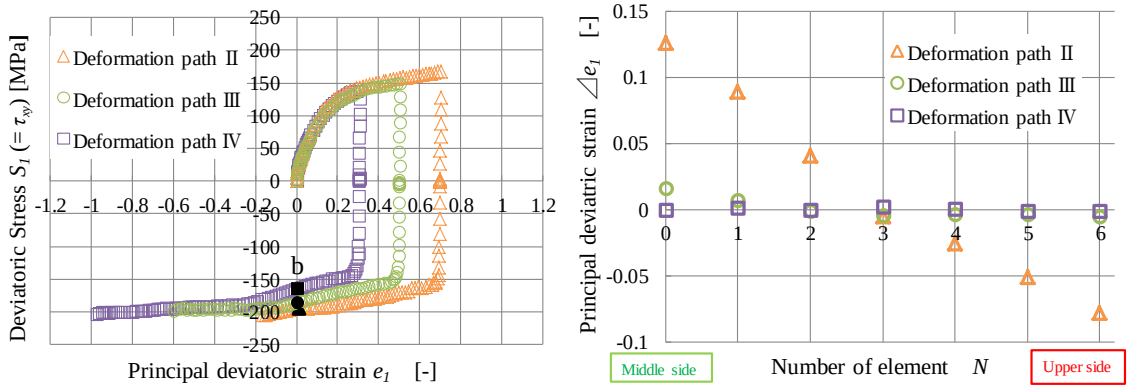

(a) Principal deviatoric stress and strain diagram. (b) Principal steain Δe_1 in each element.

Figure 4. Status of local deformation at point b.

Moreover, in order to see whether there is correlation between the local deformation and the strain history in each deformation path, the progress of local deformation is examined at point c in Figure 5 (a) where the plastic strain integrated along the deformation path becomes the same value, i.e., $\|e_1\| = 1.6$[-]. Figure 5 (b) shows the distributions of the differences of principal strain Δe_1 obtained under the condition at point c. It can be seen that since the differences of principal strain obtained by three different deformation paths are almost the same distribution, the progress

of local deformation is almost the same if the total plastic strain obtained by integrating along each deformation path is the same.

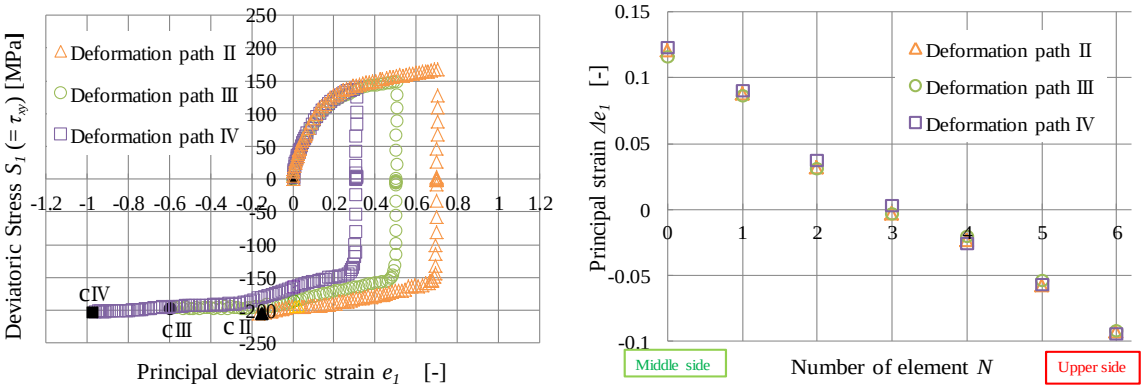

(a) Principal deviatoric stress and strain diagram.

(b) Principal steain Δe_1 in each element.

Figure 5. Status of local deformation at point c.

5 CONCLUDING REMARKS

In this study, focusing on the simple shear that the sectional shape of a test piece does not significantly change, the progress of local deformation was investigated under different deformation paths and the following results were derived.

(1) It is confirmed that since the local deformation does not occur in the final state of forward shear, the local deformation arises during the process of applying the reverse shear.

(2) The local deformation was examined at the place where the shear deformation measured by using the displacement meter becomes zero. As a result, it is revealed that the local deformation is likely to occur as the value of simple shear in the forward direction is larger.

(3) Moreover, it was revealed that the occurrence of local deformation is almost the same when the values of plastic strain obtained by integrating along each deformation path are the same value even if the deformation paths are different.

References

Kato, Y., Image Analysis Based Finite Strain Measurement of Local Deformation under Uniaxial Loading Using Natural Strain, *Implementing Innovative Ideas in Structural Engineering and Project Management*, Yazdani, S., and Singh, A (eds.), 1165-1170, *ISEC* Press, 2015.

Kato, Y., and. Futami, M., Finite Strain Measurement Based on Image Analysis using Natural Strain (Measurement and Evaluation in Uniform Deformation Field), *New Development in Structural Engineering and Construction*, *Vol 1*, Yazdani, S. and Singh, A. (eds.), 171-176, RPS Publishing, 2013.

Kato, Y., and Moriguchi, Y., Finite Deformation Analysis Using Natural Strain (on Anisotropy in Yield Surface Under Large Uni-Axial Tension and Shear), *System-Based Vision for Strategic and Creative Design*, Bontempi, F. (ed.), 669-675. Rotterdam, Balkema, 2003.